BIOFIDELITY EVALUATION FOR THE KNEE AND LEG OF THE POLAR PEDESTRIAN DUMMY

Yukou Takahashi
Honda R&D Americas, Inc.
United States
Yuji Kikuchi
Masayoshi Okamoto
Akihiko Akiyama
Honda R&D Co., Ltd.
Japan
Johan Ivarsson
Dipan Bose
Damien Subit
JaeHo Shin
Jeff Crandall
University of Virginia
United States
Paper Number 05-0280

ABSTRACT

Biofidelity of the Polar-II pedestrian dummy lower extremity was assessed in a series of dynamic bending tests relative to published PMHS (Post Mortem Human Subject) response corridors. Dynamic 4-point lateral bending tests of the knee joint and dynamic 3-point lateral bending tests of the leg from the original version of the Polar-II dummy were performed under identical test conditions to the published PMHS tests that simulated car-pedestrian lower limb impact at 40 km/h. Although the force-deflection and moment-deflection responses of the leg were found to be biofidelic, the knee joint test results showed that the stiffness in lateral bending needed to be increased. Based on the test results, a modified version of the knee joint was designed and fabricated with increased lateral bending stiffness to improve response biofidelity. The modified knee joint was evaluated in the dynamic 4-point lateral bending test, and the test results were compared with the same human response corridors. It was found that the moment-angle response of the modified knee joint in valgus bending was significantly closer to those of human subjects compared to the original version.

INTRODUCTION

Lower limb injuries account for a major part of non-fatal injuries to pedestrians. Ashton et al. [1] investigated 1560 pedestrians struck by the fronts of cars and light goods vehicles in England from 1972 to 1976, and found that more than 60% of pedestrians sustaining non-minor (AIS 2-3) injuries sustained lower limb injuries. Laumon et al. [2] investigated all the road crash victims in the department du Rhone, France, from 1995, and found that approximately one out of five pedestrian victim sustained AIS2+ lower limb injuries. Stutts et al. [3] collected patient data from eight hospital emergency rooms across the U.S., and found that approximately half of the pedestrians admitted to the emergency rooms were treated for lower limb injuries. Harruff et al. [4] examined 217 fatal pedestrian accidents in Washington State from 1990 to 1995, and identified pelvic and lower limb fractures in 66 % of the cases. Jarrett et al. [5] looked at both the Pedestrian Injury Causation Study (PICS) and the Pedestrian Crash Data Study (PCDS) databases collected by the National Highway Traffic Safety Administration (NHTSA), and the body region injury distribution showed that the lower extremity represented the most frequently injured body region in both databases. Matsui et al. [6] analyzed the pedestrian accident data collected by the Institute for Traffic Accident Research and Data Analysis (ITARDA) in Japan in 1997, and concluded that lower limb injuries accounted for 40% of all severe injuries in non-fatal accidents.

A number of past studies have focused on the development of anthropomorphic test devices for pedestrian lower limbs. Those devices can be classified into two categories – impactors for subsystem tests that represent only one single lower limb of a pedestrian, and dummies for full-scale tests that represent a whole body of a pedestrian.

The European Enhanced Vehicle-safety Committee (EEVC) Working Group 17 has specified a test procedure for legform to bumper test [7]. Based on the requirement from the EEVC Working Group 17, the Transport Research Laboratory (TRL) has developed a legform impactor [8]. Although the TRL legform impactor is one of the most widely used test devices for

assessing performance of a car front with respect to pedestrian lower limb protection, the biofidelity of its knee joint response has not been directly validated. In terms of scientific background for the knee joint stiffness requirement in static lateral bending specified in the EEVC report [7], the preceding EEVC Working Group 10 Report stated that the knee joint stiffness from the specification corridor seemed much stiffer relative to the PMHS test results by Cesari and his co-workers [9]. However, it was believed that the lower impact speed relative to the specification at which the PMHS tests were run as well as the lack of muscle force in the PMHS tests justified the higher stiffness in the specification corridor. Matsui et al. [10] validated the biofidelity of the TRL legform impactor against the impact force time history corridors developed based on the PMHS studies by Kajzer et al. [11][12]. They also used another legform impactor developed by the Japan Automobile Research Institute (JARI), and the JARI impactor was tested with two different pairs of steel knee bars in bending (one with standard 450 Nm maximum moment and the other with 100 Nm maximum moment). The impact force time history comparison showed that the 4.5 times difference in knee joint stiffness did not make a significant difference in impact force time history. This suggests that the impact force time histories obtained from Kajzer et al. are primarily determined by the inertial effects and stiffness of the impact surface rather than the stiffness of the knee joint. In order to validate the bending response of a knee joint in impact effectively, the knee joint response of a test device needed to be validated against test results using isolated PMHS knees. More recently, Konosu et al. [13][14] developed a new legform impactor called Flex-PLI that features flexible thigh and leg as well as four separate knee ligaments. They validated the dynamic response of the thigh, leg, and knee components separately by running similar tests to the PMHS component tests performed by Kerrigan et al. [15]-[17] and Bose et al. [18]. The response of each component was compared with the response corridors developed based on the PMHS tests by Ivarsson et al. [19]. Using the same test set-ups as those employed in the PMHS tests, it was confirmed that the Flex-PLI components had a reasonable level of biofidelity. It was also found from the results of their tests and other studies that the knee joint of the TRL legform was much stiffer relative to the human knee response tested at the same loading rate [13][14][19][20].

Although Konosu et al. has succeeded in developing a legform impactor for which biofidelity was validated at the component level, some of the past studies have found that the lack of upper body weight can lead to non-biofidelic responses of an impactor, particularly when a bumper hits the impactor above the knee joint level [21][22]. Thus, there is still a need for test tools that incorporate the upper body weight such as a full body pedestrian dummy. In addition, it is difficult to obtain an overall picture of the whole body kinematics using subsystem impactors, and thus a full-scale dummy is needed to investigate the effect of changes to vehicle front components on the whole body kinematics [23]. Based on this understanding, Honda R&D Co., Ltd. has developed a full-scale pedestrian dummy in collaboration with GESAC Inc. and JARI [23]-[26]. The primary goal of the development was to match the head trajectory and resultant velocity with the PMHS corridors developed based on Ishikawa et al. [27] at impact speeds of 32 km/h and 40 km/h. The latest version of the dummy, known as Polar-II, incorporates essential anthropomorphic features of a knee joint as well as a deformable tibia not only for more biofidelic head kinematics but for the biofidelity of the lower limb itself [26]. The flexible tibia was validated in quasi-static and dynamic 3-point tests. However, for the knee joint validation, Artis et al. [26] used the impact test results from Kajzer et al. [28][29], where a very similar test set-up was employed to that used for their older test series at lower impact speeds [11][12]. As noted above, it was anticipated that the contribution from the knee joint stiffness to the impact force time history was relatively small compared to the contribution from inertial properties and the stiffness of the impact surface. In order to ensure biofidelity of the knee joint bending response, some component tests using an isolated knee joint need to be performed and the results need to be validated against recently performed PMHS component tests.

In this study, the knee and leg components were taken from the Polar-II pedestrian dummy and were tested in 4-point lateral bending and 3-point lateral bending, respectively. For both tests, exactly the same test conditions were employed as those used in the PMHS component tests recently performed by Kerrigan et al. [15]-[17] and Bose et al. [18]. The test results were compared with the PMHS response corridors developed by Ivarsson et al. [19] based on the results from Kerrigan et al. [15]-[17] and Bose et al. [18]. Since the original knee joint was found to be less stiff relative to the PMHS response corridor, a modified version of the knee joint was designed and fabricated, and was subjected to the same 4-point lateral bending test.

METHODOLOGY

A series of component tests were performed at the University of Virginia Center for Applied Biomechanics using the knee joint and leg taken from the Polar-II pedestrian dummy. The tests employed the

same set-ups as those used in the PMHS tests performed by Kerrigan et al. [15]-[17] and Bose et al. [18]. Since the knee joint originally designed for the Polar-II dummy was found to be less stiff relative to the PMHS response corridors from Ivarsson et al. [19], a modified version of the knee joint with increased bending stiffness was designed, fabricated, and tested under the same test conditions.

Test Specimens

Knee Joint

The original version of the Polar-II dummy knee joint (denoted as 'original knee' hereafter) consists of the distal femur with femoral condyles and four casings for ligament springs, the tibial plateau with meniscus, four steel wire cables representing knee ligaments, and four springs providing stiffness that represents the tensile properties of the four major knee ligaments (anterior and posterior cruciate ligaments, medial and lateral collateral ligaments). The geometry of the femoral condyles and tibial plateau was based on a surgical human knee model, and was simplified with left and right symmetry. The meniscus was made thicker than the human meniscus to provide durability during impact testing. The ligament path and attachment points were also based on the surgical human knee model, and the two collateral ligaments were made symmetric with the same stiffness for simplicity. The two cruciate ligaments have the same stiffness to each other but different from that of the collateral ligaments. Figure 1 shows the anterior and lateral view of the left original knee assembly. The disassembled state of the left original knee is illustrated in Figure 2. Design details of the original knee were provided by Artis et al. [26].

The test results for the original knee in 4-point bending showed that the stiffness of the knee joint was not sufficient relative to the human knees. In order to provide more biofidelic bending response of the knee joint, it was decided to design and fabricate a modified version of the Polar-II dummy knee joint (denoted as 'modified knee' hereafter). The anterior and lateral views of the right modified knee assembly and the disassembled state of the right modified knee are shown in Figure 3 and 4, respectively. The basic structure and geometry are exactly the same as those of the original knee except that the diameter of the knee ligament springs were increased and the length of the springs were made shorter to provide stiffer bending response than that of the original knee. Aluminum spacers were placed below the springs in order to accommodate the shorter springs in the spring housings.

Leg

The tibia shaft consists of a nyron/kevlar rod surrounded by a hard urethane hollow rod. The proximal and distal ends of the tibia shaft were reinforced by the inner and outer steel rings that were bonded to the tibia to provide an interface with the upper and lower tibia load cell [26]. The stiffness and damping characteristics of the skin and flesh surrounding the tibia shaft were determined from the computer simulations performed by Huang et al. [25] For the flesh, Confor foam is used for appropriate damping. The shape of the tibia shaft has been reported as tapered at the proximal and distal ends in previous papers [23][26]. However, it was decided after a number of full-scale tests to further modify the shape of the tibia shaft in such a way that the cross section of the shaft along its long axis is uniform in order to provide increased durability. Figure 5 illustrates the tibia shaft and surrounding flesh/skin of the Polar-II

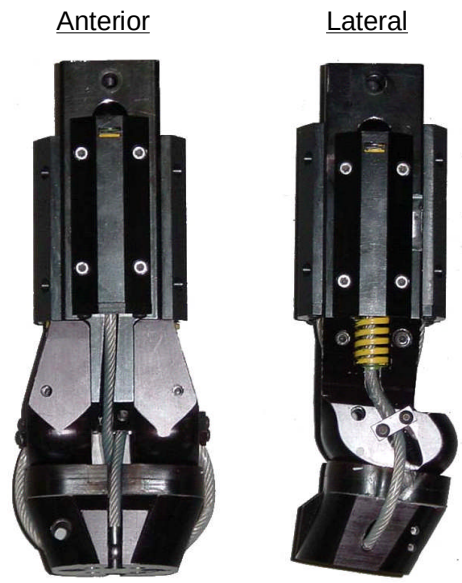

Figure 1. Anterior and lateral view of original knee joint (left knee).

Figure 2. Disassembled original knee joint (left knee).

dummy tested in this study.

Test Conditions

The original and modified versions of the knee joint from the Polar-II pedestrian dummy were subjected to valgus bending with the 4-point bending test set-up used by Bose et al. [18] for their PMHS tests with isolated knee joints. The leg (tibia shaft with surrounding flesh/skin) from the Polar-II dummy was tested in 3-point bending with the test configuration described in Kerrigan et al. [15]-[17].

Knee Joint Test

The 4-point knee bending test configuration used in this study is illustrated in Figure 6. The knee joint was attached to cylindrical aluminum hollow shafts through aluminum adaptors. The aluminum shafts were attached to support pillars through frictionless pin joints that only allow varus-valgus bending of the knee joint. The support pillar on the tibia side of the knee joint was rigidly fixed to the ground, while the pillar on the femur side was fixed to the ground through a linear bearing that allows translation in the superior-inferior direction of the knee joint in order to achieve simply supported boundary conditions. An impactor fork with two prongs was used to load the aluminum shafts to provide a 4-point bending test configuration. The fork was attached to the actuator of a displacement-controlled servo-hydraulic test machine (Instron 8874) though a frictionless pin joint. The contact surfaces between the prongs of the fork and the aluminum shafts were greased to minimize friction. The knee joint was oriented in such a way that it was subjected to valgus bending, and the initial orientation of the knee joint was set at zero degrees of the flexion-extension, varus-valgus, and axial rotation angles.

The actuator of the test machine was instrumented with a load cell and a displacement transducer to measure applied load and displacement. Three-axis load cells were used to measure reaction forces in the support pillars. A six-axis load cell was mounted between the aluminum shaft and the adaptor on the femur side of the knee joint. A triaxial accelerometer was mounted on the load cell to measure the accelerations necessary for the inertial compensation technique used for estimating the knee joint moment. Magneto-hydrodynamic (MHD) angular rate sensors were mounted on both sides of the knee joint to obtain knee bending angle time histories by time-integrating the MHD signals. A still image of a typical 4-point knee joint bending test configuration is presented in Figure 7.

Two quasi-static and three dynamic tests were run for each of the knee joints tested (original and modified

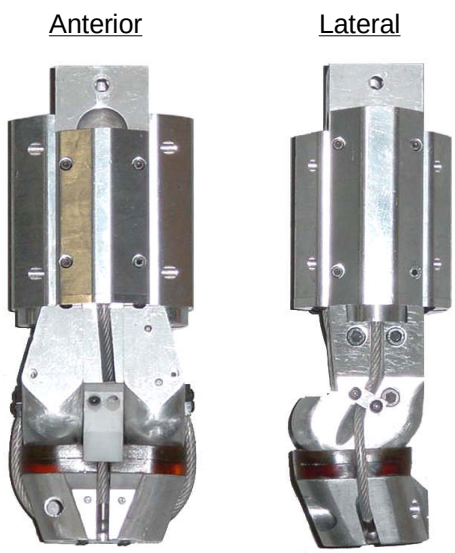

Figure 3. Anterior and lateral view of modified knee joint (right knee).

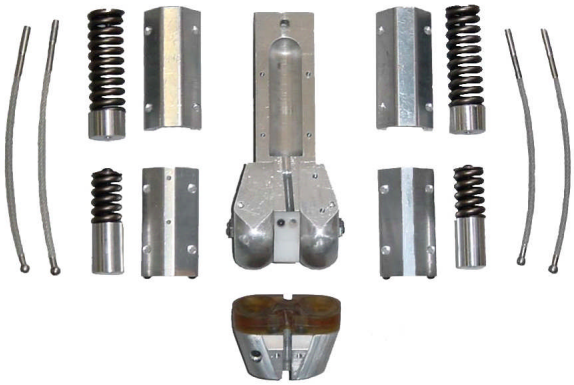

Figure 4. Disassembled modified knee joint (right knee).

Figure 5. Tibia shaft and leg flesh/skin.

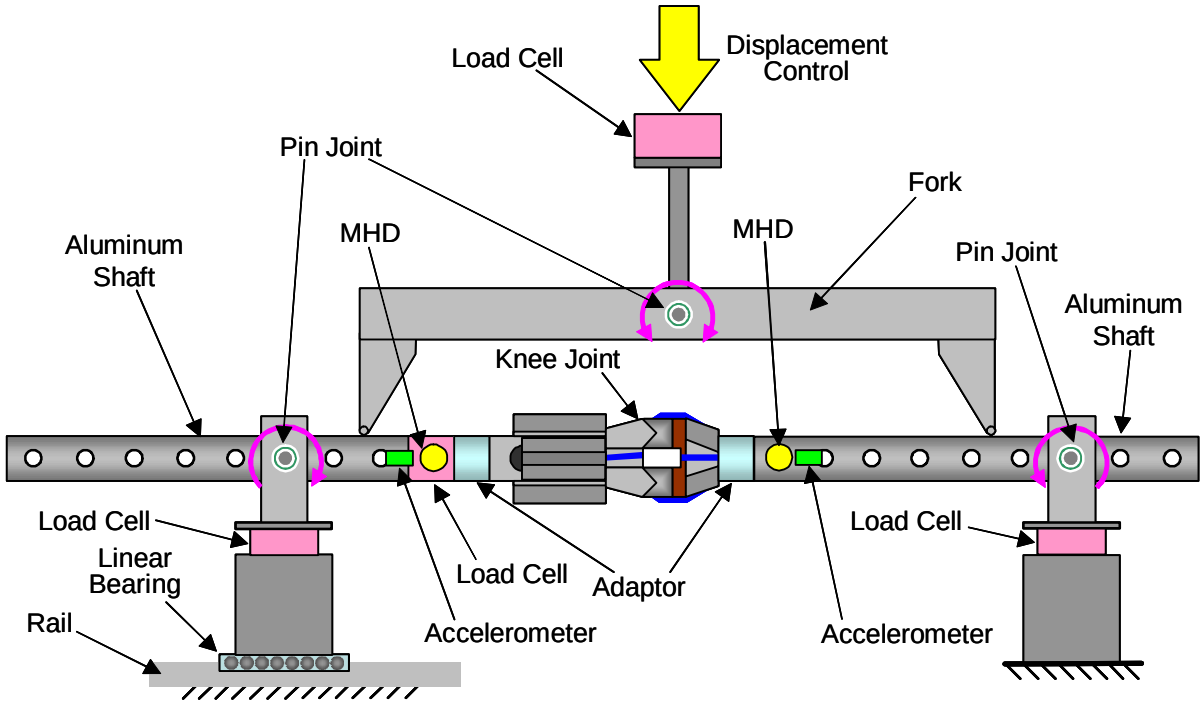

Figure 6. Schematic diagram of 4-point knee bending test configuration.

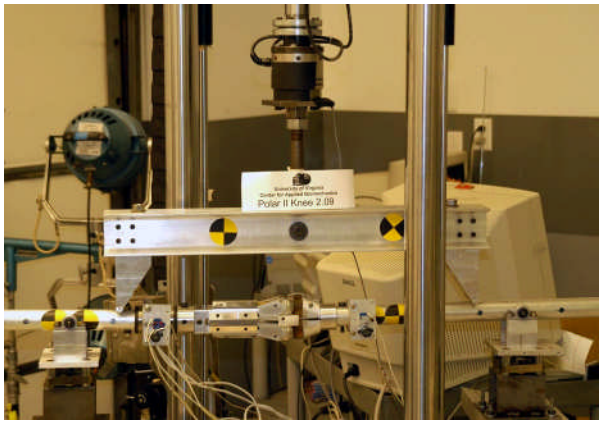

Figure 7. Typical 4-point knee bending test set-up.

knees). Bose et al. [18] investigated previous studies that provided knee bending angle time histories using PMHS lower limbs or legform impactors and found that the bending rate was approximately 1.0 degrees/ms in impacts at 40 km/h. Based on this observation, they decided to use the rate of 1.0 degrees/ms in their dynamic bending tests of isolated PMHS knees. In this study, the same knee bending rate was used in the dynamic tests in order to enable direct comparison with the PMHS test results. The target displacement rate was then determined using a simple geometric analysis. The knee bending rate for the quasi-static tests was approximately 1.0 degrees/s. The maximum knee bending angle was set at 20 degrees for the quasi-static tests and 15 degrees for the dynamic tests in order to enable comparisons of the test results with the PMHS corridor by Ivarsson et al. [19] up to the maximum bending angle of the average PMHS response.

Leg Test

A schematic of the 3-point leg bending test configuration is shown in Figure 8. Aluminum cylindrical adaptors were rigidly attached to both ends of the deformable tibia shaft. These adaptors were mounted on aluminum disks that were in turn rigidly attached to half-cylindrical solid aluminum rollers. The diameter of the rollers was exactly the same as that of the rollers used in the PMHS tests performed by Kerrigan et al. [15]-[17]. The rollers were placed on the support plates, and the contact surfaces between the rollers and support plates were greased to minimize friction at the contact points. The same test machine as that used for the knee joint test (Instron 8874) was used to load the leg specimen in the lateromedial direction. A rigid impactor that loaded the leg specimen at mid-span had a circular tip and was attached to the actuator of the test machine. The location of the mid-span loading point relative to the tibia shaft was determined in such a way that the point corresponded to the midpoint between the knee joint and the ankle joint in the dummy. In the dummy leg assembly, the tibia shaft is not positioned exactly in the middle of the knee joint and the ankle joint. Therefore, the mid-span loading point defined and used in the current study did not correspond to the mid-shaft of the tibia. This can be confirmed on an example still image of the leg bending test configuration shown in Figure 9 by comparing the

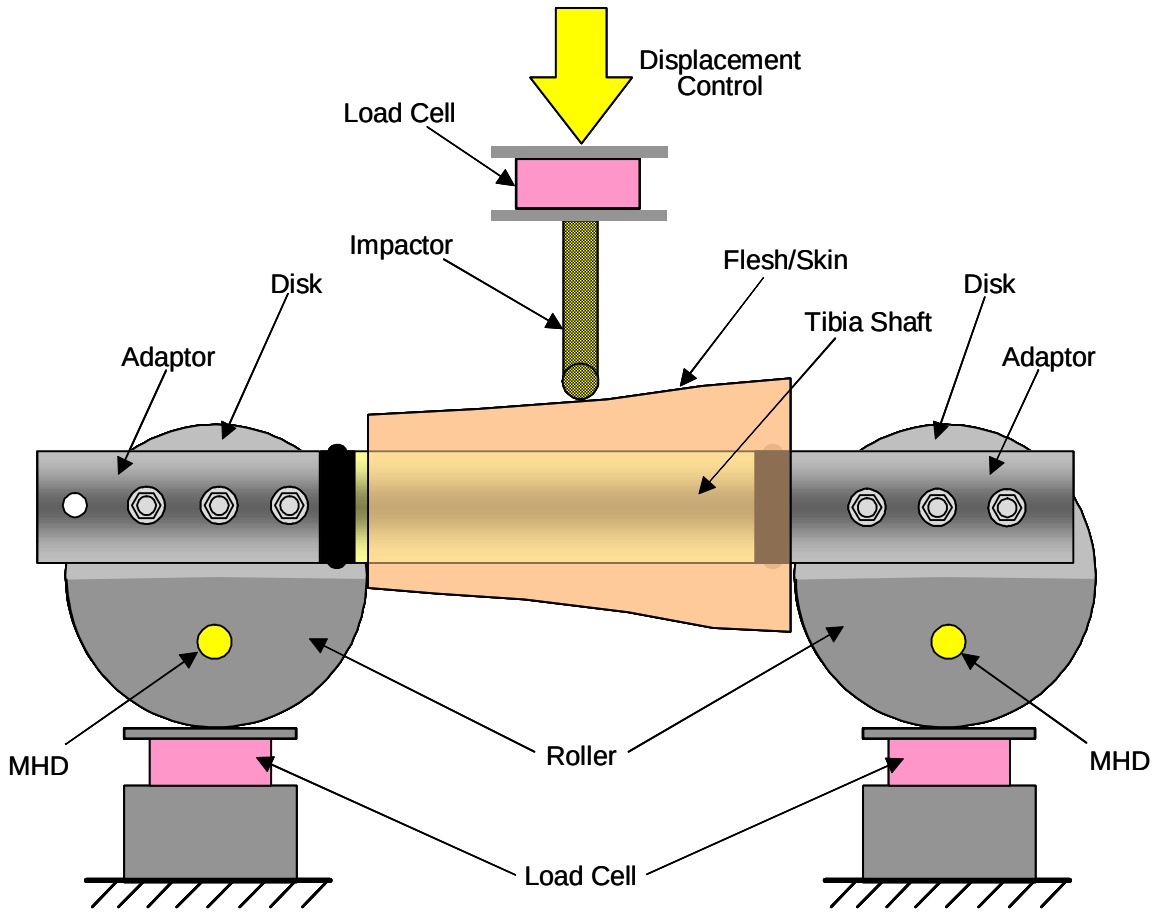

Figure 8. Schematic diagram of 3-point leg bending test configuration.

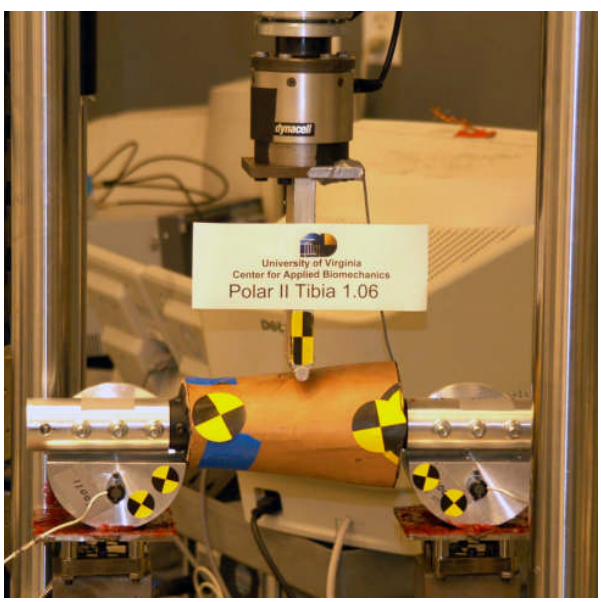

Figure 9. Typical 3-point leg bending test set-up.

position of the steel rings (in black) relative to the rollers (see also Figure 8). The leg flesh/skin for the Polar-II dummy was placed around the tibia shaft in order to obtain the overall leg bending response. The portion of the leg flesh/skin that corresponds to the superior-inferior range of the tibia shaft in the dummy was cut out from the intact leg flesh/skin assembly in such a way that it fitted between the rollers. The 3-point bending span length was set at 334 mm to which Ivarsson et al. [19] scaled the PMHS test results in order to obtain response corridors scaled to the size of a 50th percentile adult male.

A load cell was mounted between the actuator and the impactor to measure applied load. Three-axis load cells were placed underneath the support plates to obtain reaction forces. Angular velocities of the rollers were measured by the MHD angular rate sensors affixed to the rollers.

Two quasi-static and three dynamic tests were conducted using the tibia shaft of the dummy surrounded by the flesh/skin. For the dynamic tests, the loading rate was set at approximately 1.5 m/s. This loading rate was chosen so that the test results could be directly compared with the PMHS test results by Kerrigan et al. [15]-[17]. The loading rate for the quasi-static tests was approximately 1.0 mm/s.

RESULTS

Ivarsson et al. [19] presented PMHS response corridors for the mid-span 3-point leg bending in the lateromedial direction as well as the 4-point knee valgus bending. The force-deflection and moment-deflection corridors and the moment-angle corridor (all scaled to a 50th percentile adult male anthropometry) were presented for the leg bending and the knee bending, respectively. In order to compare the test results obtained in this study with the PMHS response corridors, the moment-angle response of the knee joint and the force-deflection and moment-deflection responses of the leg were calculated from the signals obtained in the tests.

Knee Joint Test

For the dynamic knee bending tests, Bose et al. [18] estimated forces and moments at the knee joint from the loading environment measured by the load cell installed near the knee joint using an inertial compensation procedure, and the results were used to develop the response corridors by Ivarsson et al. [19]. In this study, the same inertial compensation procedure as that used by Bose et al. [18] was employed to calculate moment at the knee joint. Figure 10 shows a free body diagram of the superior part of the knee joint (proximal knee segment) in the coronal plane. The equations of motion of the knee segment about its center of gravity in tangential (lateromedial) translation and rotation in the coronal plane are given by Equation 1 and 2:

$$M\ddot{u} = V_K - V_F \qquad (1).$$

$$I\ddot{\theta} = M_F - M_K + V_F x_F + V_K x_K \qquad (2).$$

Since the distal half of the load cell is included in the knee segment, M_F and V_F are given by the load cell signals. Thus, the moment at the knee joint, M_K, can be

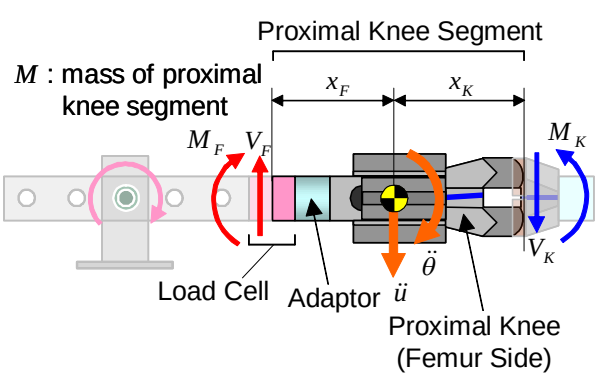

Figure 10. Free body diagram for proximal knee segnemt.

calculated using Equation 3:

$$M_K = M_F + V_F(x_F + x_K) + M\ddot{u}x_K - I\ddot{\theta} \qquad (3).$$

Since the test configuration was intended to provide 4-point bending of the knee joint, V_F was expected to be minimal in the quasi-static tests. However, the test results showed that V_F increases as the knee valgus bending angle goes up. The magnitude of V_F at the knee valgus angle of 15 degrees was approximately 40 N and 70 N for the original knee joint and the modified knee joint, respectively. Since the moment component in Equation 3 generated by those forces corresponded to 17% and 13% of the magnitude of M_F for the original knee joint and the modified knee joint, respectively, it was decided that the effect of V_F on the moment at the knee joint M_K be taken into account, rather than simply using M_F for M_K.

In order to calculate the moment at the knee joint using Equation 3, the moment of inertia and the center of gravity location for the portion between the center of the load cell and the distal end of the femoral condyles of the knee joint (proximal knee segment: Figure 10) were measured using a torsional pendulum (Inertia Dynamic Inc.). Table 1 summarizes the inertial property values measured for the original and modified knee joints. The linear acceleration in Equation 3 was measured by the accelerometer mounted on the load cell. The angular acceleration in Equation 3 was calculated from the accelerometer signal divided by the distance between the support pin joint and the accelerometer.

Figures 11 and 12 plot moment-angle responses at the knee joint calculated using Equation 3 for the original knee joint and the modified knee joint, respectively, in both quasi-static and dynamic valgus bending. In the quasi-static condition, the moment-angle response is fairly linear for both the original knee joint and the stiffer knee joint. However, significant oscillation of moment-angle response is seen in the dynamic condition, particularly for the original knee joint. This oscillation was identified after the dynamic bending tests of the original knee joint. Since the natural frequency estimated using the knee bending stiffness from the quasi-static tests and the inertial

Table 1.
Inertial properties of proximal knee segments.

Knee	Mass (kg)	MOI (kgm²)	x_F (m)	x_K (m)
Original	2.12	0.01362	0.1238	0.1345
Modified	2.48	0.01397	0.1225	0.1358

(MOI: Moment of Inertia)

properties of the knee and fixtures was much lower than that of the oscillation observed in the moment-angle response, it was assumed before the modified knee joint testing that this oscillation came from the stiffness of the fixtures themselves combined with the stiffness of the connecting portions between the fixtures. Based on this assumption, special attention was paid to increase the rigidity of the connections between the fixtures when setting up for the modified knee joint testing. Since this effort resulted in much lower magnitude of oscillations observed in the moment-angle response of the modified knee joint, it was concluded that the above-mentioned assumption was valid, and that the response of the knee joint itself can be extracted from the oscillated signals by simply eliminating the oscillation. Therefore, the moment-angle response was post-processed in order to eliminate unfavorable oscillations and compare the results with the published PMHS response corridor.

Two different post-processing procedures were used to try to eliminate the oscillation – filtering and curve-fitting. For filtering, each term of Equation 3 was filtered at CFC 60, and then the moment at the knee joint was calculated using the filtered signals. For curve-fitting, unfiltered signals were used to calculate the moment at the knee joint using Equation 3, and then polynomial regression was applied to the moment-angle curves. Figures 13 and 14 plot the results of filtering and curve-fitting for the moment-angle response of the original knee and the stiffer knee, respectively. The filtered moment-angle curves for the original knee joint presented in Figure 13 show unrealistic bending characteristics such as the initial negative moment and strong nonlinearity. Since the

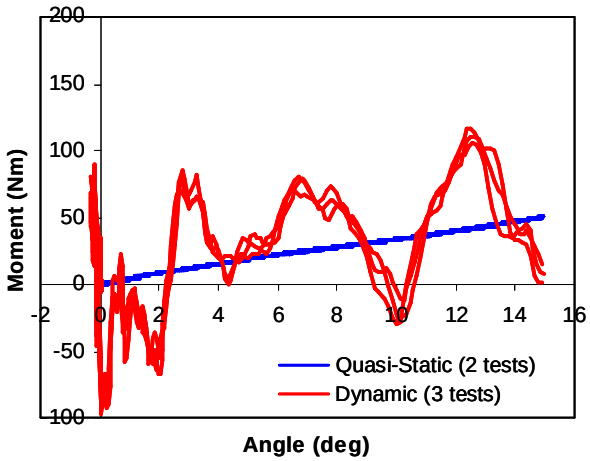

Figure 11. Quasi-static and dynamic moment-angle responses at knee joint for original knee joint.

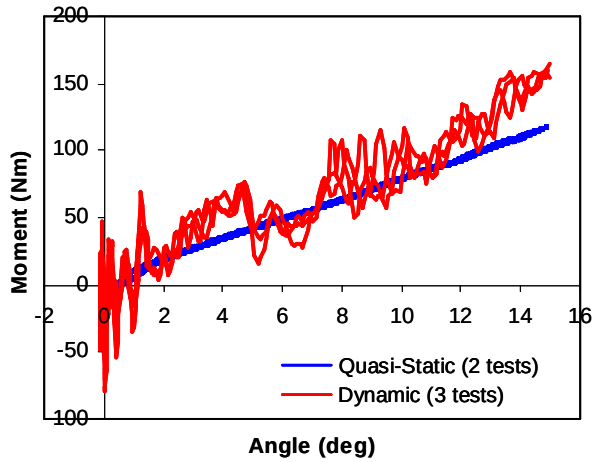

Figure 12. Quasi-static and dynamic moment-angle responses at knee joint for modified knee joint.

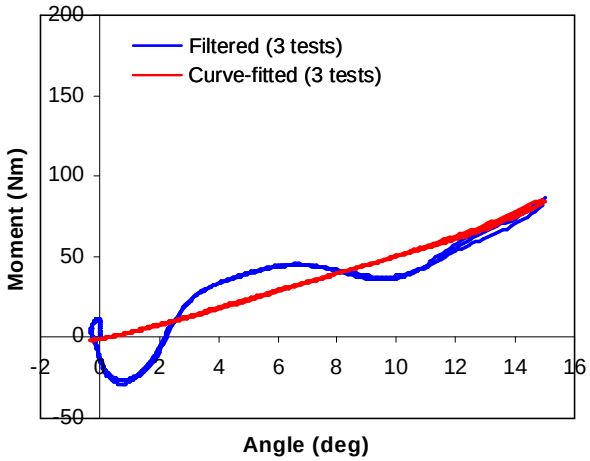

Figure 13. Filtered and curve-fitted dynamic moment-angle responses at knee joint for original knee joint.

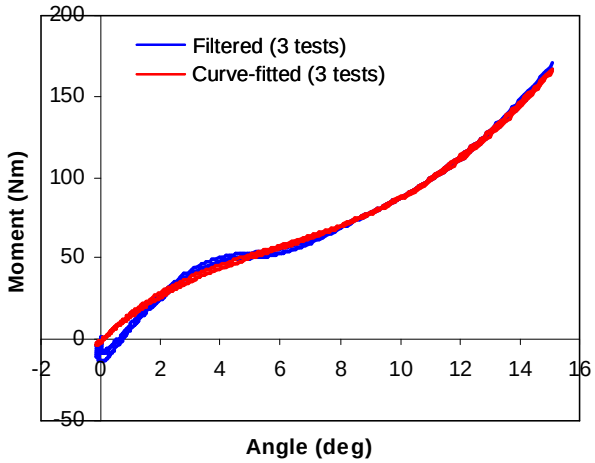

Figure 14. Filtered and curve-fitted dynamic moment-angle responses at knee joint for modified knee joint.

unfiltered moment-angle response for the modified knee joint demonstrates much smaller magnitude of oscillation than that of the original knee joint, the filtered moment-angle curves for the modified knee joint look more realistic (Figure 14). However, the initial negative moment is still seen, although the magnitude is much smaller. Considering the fact that the moment-angle response of both knee joints in quasi-static valgus bending is fairly linear, it can be concluded that the curve-fitting procedure does a better job compared to the CFC 60 filtering to extract characteristics of the knee joint valgus bending response from the oscillated signals.

Leg Test

In order to compare the 3-point bending test results with the PMHS response corridors presented by Ivarsson et al. [19], force-deflection and moment-deflection curves were determined using the signals obtained from the tests. Although the applied force can be measured by the load cell mounted above the impactor, summation of vertical support forces from both support load cells was used to determine the applied force in order to avoid the problem of inertial contribution from mass acceleration. Since the mid-span of the leg specimen was loaded, the moment can be calculated in three ways: $FL/4$, $F_1L/2$, and $F_2L/2$, where F_1 is the vertical component of the reaction force on one support, F_2 is the vertical component of the reaction force on the other support, L is the span length, and $F = F_1+F_2$. Figure 15 plots the moment-deflection curves from the three different methods for moment calculation for one of the three dynamic 3-point bending tests. In spite of the fact that the mid-span loading configuration defined in this study resulted in asymmetric loading to the tibia shaft, it was found in Figure 15 that the effect of the asymmetry on the moment calculation was so small that the three different methods for moment calculation yielded almost the same moment-deflection curves. Thus, it was decided to use $FL/4$ for moment calculation for simplicity. Figures 16 and 17 show the force-deflection and moment-deflection curves, respectively, obtained from the quasi-static and dynamic 3-point bending tests. The initial toe region with lower stiffness primarily represents the deflection of the flesh/skin surrounding the tibia shaft, and the successive region with higher stiffness corresponds mainly to the bending stiffness of the tibia shaft. For the dynamic tests, some oscillation is observed in the force-deflection and moment-deflection. However, the magnitude of the oscillation is smaller with lower frequency relative to the oscillation seen in the dynamic knee bending tests. Thus, it was decided not

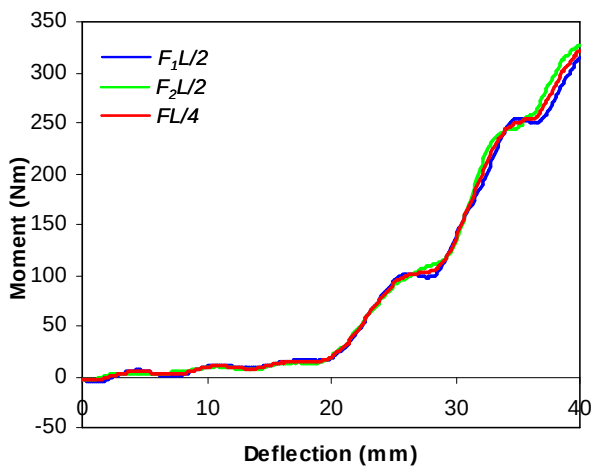

Figure 15. Moment-deflection response from three different methods for moment calculation.

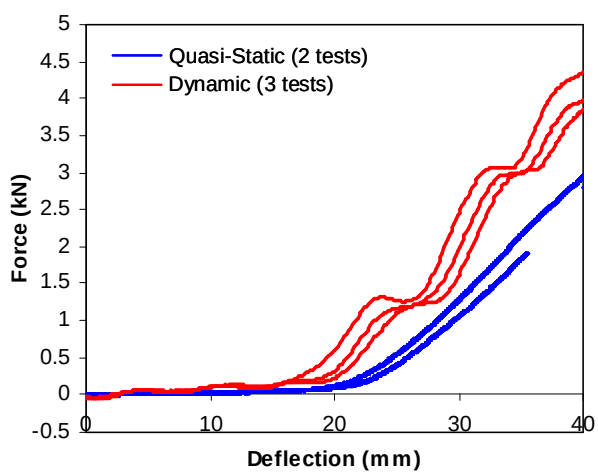

Figure 16. Quasi-static and dynamic force-deflection response of leg.

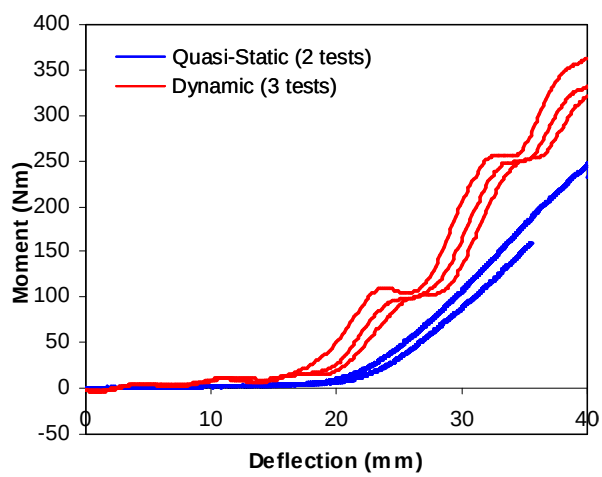

Figure 17. Quasi-static and dynamic moment-deflection response of leg.

to filter or curve-fit the curves for diminishing the oscillation.

DISCUSSION

Since Ivarsson et al. [19] shows scaled PMHS response corridors for the knee and leg test in dynamic condition, only the results from the dynamic tests were compared with the PMHS corridors. Figure 18 compares the moment-angle response at the knee joint between the dummy tests conducted in this study and the PMHS response corridor for a 50th percentile adult male from Ivarsson et al. [19]. Both filtered and curve-fitted response curves were included in the figure. It is obvious that the original knee joint is less stiff than the human knee, with moment-angle curves falling below the lower bound of the PMHS corridor. The curves for the modified knee joint fell almost perfectly within the PMHS corridor except for the artificial initial negative moment in the filtered curves. Figures 19 and 20 compare the force-deflection and moment-deflection responses of the leg, respectively, between the dummy tests and the PMHS corridors. The initial toe region for the dummy leg seems to be longer than that of the PMHS corridors probably due to the difference in thickness of the surrounding flesh between the dummy and PMHS legs. Other than that, all the curves from the dummy leg tests almost fell within the PMHS response corridors.

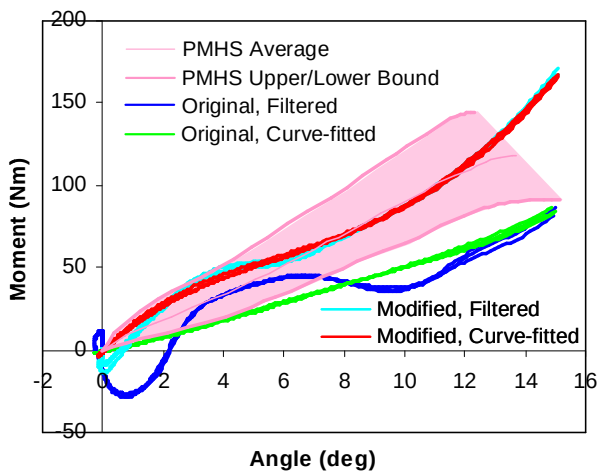

Figure 18. Comparison of moment-angle response of knee between PMHS and dummy.

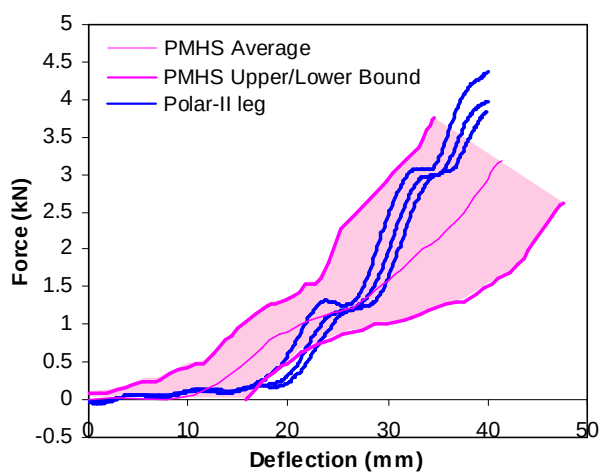

Figure 19. Comparison of force-deflection response of leg between PMHS and dummy.

In order to quantitatively assess the biofidelity of the knee joint and leg of the Polar-II pedestrian dummy tested, the Response Measurement Comparison Value defined by Rhule et al. [30] was calculated for each dynamic test. Figure 21 illustrates the definitions of the Dummy Variance (DV) and Cadaver Variance (CV) presented by Rhule et al. [30]. Although they defined CV and DV for independent variables as functions of time, it was decided to apply this definition directly to the moment-angle curves of the knee joint as well as the force-deflection and moment-deflection curves of the leg since both the PMHS and dummy tests employed the displacement-controlled test machine and thus displacement time histories were prescribed independently from the response of the test specimens. The Dummy Cumulative Variance (*DCV*), Cadaver Cumulative Variance (*CCV*), and Response Measurement Comparison Value (*R*) were then defined by the following formulae:

$$DCV = \sum_{d=0}^{n} DV(d)^2 \qquad (4).$$

$$CCV = \sum_{d=0}^{n} CV(d)^2 \qquad (5).$$

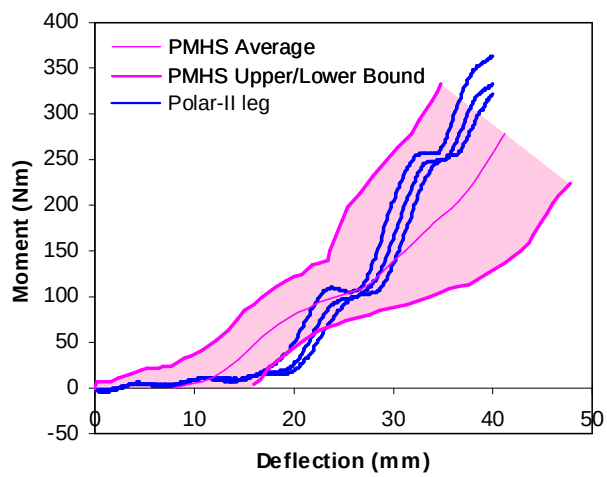

Figure 20. Comparison of moment-deflection response of leg between PMHS and dummy.

$$R = DCV / CCV \qquad (6).$$

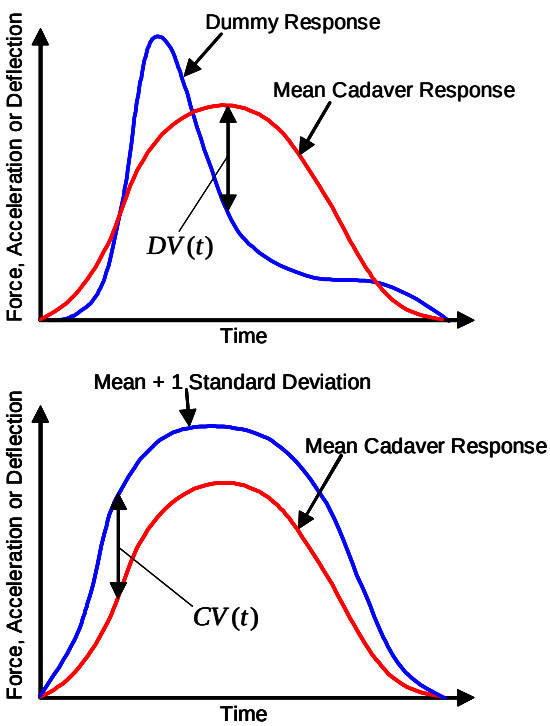

Figure 21. Dummy Variance (DV) and Cadaver Variance (CV) (Rhule et al. [30]).

where d represents either knee bending angle or leg mid-span deflection. Therefore, $R^{1/2}$ represents cumulative dummy variance relative to the mean cadaver response normalized by the cumulative cadaver response variance relative to the mean cadaver response. Thus, if $R^{1/2}$ is less than 1.0, then the cumulative dummy variance is less than the cumulative cadaver variance (both relative to the mean cadaver response) and the biofidelity of the specimen tested can be considered to be very good.

Tables 2 and 3 summarize the results of $R^{1/2}$ calculations for the dynamic knee joint and leg tests, respectively. In terms of the knee joint tests, both filtered and curve-fitted moment-angle curves were subjected to the calculation. The response corridors presented in Ivarsson et al. were developed around the characteristic average response using standard deviation calculations for both the independent and dependent variables [19]. Due to the technique used for the corridor development, the upper and lower bounds do not have the same distance in the vertical direction from the mean response. Thus, both upper and lower bounds were used in calculating *CCV*, and average *CCV* was calculated for each response corridor. $R^{1/2}$ for the original knee joint was between one and two for both filtered and curve-fitted moment-angle curves, while the modified knee joint resulted in $R^{1/2}$ values of less than 0.4 for both post-processing methods. $R^{1/2}$ for

Table 2.
$R^{1/2}$ calculation for bending of original and modified knee with two different signal post-processing methods and two different CCV calculations (upper/lower bound).

Specimen	Test #	Moment-Angle / Filtered			Moment-Angle / Curve-Fitted		
		Upper	Lower	Average	Upper	Lower	Average
Original Knee	1	1.342	1.792	1.567	1.142	1.525	1.333
	2	1.354	1.808	1.581	1.138	1.520	1.329
	3	1.350	1.803	1.576	1.134	1.514	1.324
	Average	1.349	1.801	1.575	1.138	1.520	1.329
Modified Knee	1	0.292	0.390	0.341	0.234	0.312	0.273
	2	0.343	0.458	0.400	0.292	0.391	0.341
	3	0.304	0.406	0.355	0.236	0.315	0.276
	Average	0.313	0.418	0.366	0.254	0.339	0.297

Table 3.
$R^{1/2}$ calculation for bending of leg with two different signal post-processing methods and two different CCV calculations (upper/lower bound).

Specimen	Test #	Force-Deflection			Moment-Deflection		
		Upper	Lower	Average	Upper	Lower	Average
Leg	1	0.455	0.889	0.672	0.429	0.856	0.642
	2	0.490	0.958	0.724	0.447	0.892	0.669
	3	0.580	1.132	0.856	0.513	1.026	0.769
	Average	0.508	0.993	0.751	0.463	0.925	0.694

the force-deflection and moment-deflection of the leg were less than one. Those results suggest that the biofidelity of the modified knee joint and the leg from the Polar-II dummy in lateral bending is very good at the component level.

Although the modified knee joint and leg of the Polar-II pedestrian dummy were found to be biofidelic, they are not currently designed to fail during impact testing. On the other hand, a human knee and/or leg may fail particularly when a pedestrian is subjected to severe impact conditions. Since the failure to the knee and/or leg may affect the upper body kinematics of a pedestrian in a car-pedestrian impact, future study needs to quantify the effect of the responses of the knee and leg components on the upper body kinematics of the dummy in full-scale testing.

CONCLUSION

In this study, a series of component tests using the original and modified knee joint and the leg from the Polar-II pedestrian dummy were conducted. Based on the results of the tests, the following conclusions were reached.

1. Limited rigidity in the test fixtures resulted in unfavorable oscillation in the moment-angle response of the knee joint.
2. Polynomial regression yielded a better representation of the knee joint bending characteristics from noisy moment-angle curves relative to low-pass filtering.
3. The original knee joint of the Polar-II dummy was found to be less stiff than the human knee in valgus bending ($R^{1/2}$=1.33 with curve-fitted moment-angle response).
4. The modified knee joint of the Polar-II dummy with increased stiffness of the ligament springs exhibited very biofidelic response in valgus bending ($R^{1/2}$=0.30 with curve-fitted moment-angle response).
5. The leg (deformable tibia shaft with flesh/skin) of the Polar-II dummy yielded very biofidelic force-deflection and moment-deflection responses in lateromedial 3-point bending ($R^{1/2}$=0.75 for force-deflection and 0.69 for moment-deflection).
6. Future study needs to quantify the effect of the knee and leg responses on the upper body kinematics of the dummy in full-scale testing.

REFERENCES

[1] Ashton S., Pedder J., Mackay G., "Influence of Vehicle Design on Pedestrian Leg Injuries", Proceedings of the 22nd Annual Conference of the American Association of Automotive Medicine, 1978.

[2] Laumon B., Martin J., Collet P., Chiron M., Vemey M., NDiaye A., Vergnes I., "A French Road Accident Trauma Registry: First Results", Proceedings of the 41st Annual Conference of the American Association of Automotive Medicine, 1997.

[3] Stutts J., "Injuries to Pedestrians and Bicyclists: A Look at Non-Motor Vehicle and Non-Roadway Events", Proceedings of the 41st Annual Conference of the American Association of Automotive Medicine, 1997.

[4] Harruff R., Avery A., Alter-Pandya A., "Analysis of Circumstances and Injuries in 217 Pedestrian Traffic Fatalities", Accident Analysis and Prevention, Vol. 30, No. 1, 1998.

[5] Jarrett K., Saul R., "Pedestrian Injury – Analysis of the PCDS Field Collision Data", 16th ESV Conference, Paper Number 98-S6-O-04, 1998.

[6] Matsui Y., Ishikawa H., Sasaki A., "Pedestrian injuries Induced by the Bonnet Leading Edge in Current Car-Pedestrian Accidents", SAE Paper 1999-01-0713, 1999.

[7] European Enhanced Vehicle-safety Committee, "EEVC Working Group 17 Report; Improved Test Methods to Evaluate Pedestrian Protection Afforded by Passenger Cars", www.eevc.org, 1998.

[8] Laurence G., Hardy B., "Pedestrian Safety Testing Using the EEVC Pedestrian Impactors", 16th ESV Conference, Paper Number 98-S10-O-03, 1998.

[9] European Experimental Vehicles Committee, "EEVC Working Group 10 Report; Proposals for methods to evaluate pedestrian protection for passenger cars", 1994.

[10] Matsui Y., Ishikawa H., Sasaki A., Kajzer J., Schroeder G., "Impact Response and Biofidelity of Pedestrian Legform Impactors", IRCOBI Conference, 1999.

[11] Kajzer J., Cavallero C., Ghanouchi S., Bonnoit J., Ghorbel A., "Response of the Knee Joint in Lateral Impact – Effect of Shearing Loads", IRCOBI Conference, 1990.

[12] Kajzer J., Cavallero C., Bonnoit J., Morjane A., Ghanouchi S., "Response of the Knee Joint in Lateral Impact – Effect of Bending Moment", IRCOBI Conference, 1993.

[13] Konosu A., Tanahashi M., "Development of a Biofidelic Flexible Pedestrian Legform Impactor", Stapp Car Crash Journal, Vol. 47, 2003.

[14] Konosu A., Issiki T., Tanahashi M., "Development of a Biofidelic Flexible Pedestrian Leg-form Impactor (Flex-PLI 2004) and Evaluation of its Biofidelity at the Component Level and at the Assembly Level", SAE Paper Number 05B-161, 2005.

[15] Kerrigan J., Bhalla K., Madeley N., Funk J., Bose D., Crandall J., "Experiments for Establishing Pedestrian-Impact Lower Limb Injury Criteria", SAE Paper Number 2003-01-0895, 2003.

[16] Kerrigan J., Bhalla K., Madeley N., Crandall J.,

Deng B., "Response Corridors for the Human Leg in 3-point Lateral Bending", The 7th USA National Congress on Computational Mechanics, 2003.
[17] Kerrigan J., Drinkwater C., Kam C., Murphy D., Ivarsson J., Crandall J., "Tolerance of the Human Leg and Thigh in Dynamic Lateral-Medial 3-point Bending", the 2004 International Crashworthiness Conference, 2004.
[18] Bose D., Bhalla K., van Rooij L., Millington S., Studley A., Crandall J., "Response of the Knee Joint to the Pedestrian Impact Loading Environment", SAE Paper Number 2004-01-1608, 2004.
[19] Ivarsson J., Lessley D., Kerrigan J., Bhalla K., Bose D., Crandall J., Kent R., "Dynamic Response Corridors and Injury Thresholds of the Pedestrian Lower Extremities", IRCOBI Conference, 2004.
[20] Bhalla K., Bose D., Madeley J., Kerrigan J., Crandall J., Longhitano D., Takahashi Y., "Evaluation of the Response of Mechanical Pedestrian Knee Joint Impactors in Bending and Shear Loading", 18th ESV Conference, 2003.
[21] Cesari D., Alonzo F., Matyjewski M., "Subsystem Test for Pedestrian Lower Leg and Knee Protection", 13th ESV Conference, Paper Number S3-O-08, 1991.
[22] Takahashi Y., Kikuchi Y., "Biofidelity of Test Devices and Validity of Injury Criteria for Evaluating Knee Injuries to Pedestrians", 17th ESV Conference, Paper Number 373, 2001.
[23] Akiyama A., Okamoto M., Rangarajan N., "Development and Application of the New Pedestrian Dummy", 17th ESV Conference, Paper Number 463, 2001.
[24] Akiyama A., Yoshida S., Matsuhashi T., Rangarajan N., Shams T., Ishikawa H., Konosu A., "Development of Simulation Model and Pedestrian Dummy", SAE Paper Number 1999-01-0082, 1999.
[25] Huang T., McDonald J., Artis M., Rangarajan N., Shams T., White Jr. R., Beach D., Campbell Jr. R., Akiyama A., Yoshida S., Ishikawa H., Konosu A., "Development of a Biofidelic Dummy for Car-Pedestrian Accident Studies", IRCOBI Conference, 1999.
[26] Artis M., McDonald J., White R., Huang T., Shams T., Rangarajan N., Akiyama A., Okamoto M., Yoshizawa R., Ishikawa H., "Development of a New Biofidelic Leg for Use With a Pedestrian Dummy", IRCOBI Conference, 2000.
[27] Ishikawa H., Kajzer J., Schroeder G., "Computer Simulation of the Impact Response of the Human Body in Car-Pedestrian Accidents", 37th Stapp Car Crash Conference, 1993.
[28] Kajzer J., Schroeder G., Ishikawa H., Matsui Y., Bosch U., "Shearing and Bending Effects at the Knee Joint at High Speed Lateral Loading", 41st Stapp Car Crash Conference, 1997.
[29] Kajzer J., Matsui Y., Ishikawa H., Schroeder G., Bosch U., "Shearing and Bending Effects at the Knee Joint at Low Speed Lateral Loading", SAE Paper Number 1999-01-0712, 1999.
[30] Rhule H., Maltese M., Donnelly B., Eppinger R., "Development of a New Biofidelity Ranking System for Anthropomorphic Test Devices", Stapp Car Crash Journal, Vol. 46, 2002.